

10-30-2016

Haploinsufficiency of the Myc regulator Mtbp extends survival and delays tumor development in aging mice.

Brian C. Grieb

Vanderbilt University Medical Center

Kelli Boyd

Vanderbilt University Medical Center

Ramkrishna Mitra

Thomas Jefferson University, ramkrishna.mitra@jefferson.edu

Christine M. Eischen

Thomas Jefferson University, christine.eischen@jefferson.edu

[Let us know how access to this document benefits you](#)

Follow this and additional works at: <https://jdc.jefferson.edu/cbfp> Part of the [Oncology Commons](#)

Recommended Citation

Grieb, Brian C.; Boyd, Kelli; Mitra, Ramkrishna; and Eischen, Christine M., "Haploinsufficiency of the Myc regulator Mtbp extends survival and delays tumor development in aging mice." (2016).

Department of Cancer Biology Faculty Papers. Paper 106.<https://jdc.jefferson.edu/cbfp/106>

Haploinsufficiency of the Myc regulator Mtbp extends survival and delays tumor development in aging mice

Brian C. Grieb¹, Kelli Boyd¹, Ramkrishna Mitra², Christine M. Eischen^{1,2}

¹Department of Pathology, Microbiology and Immunology, Vanderbilt University Medical Center, Nashville, TN 37212, USA

²Department of Cancer Biology, Sidney Kimmel Cancer Center, Thomas Jefferson University, Philadelphia, PA 19107, USA

Correspondence to: Christine M. Eischen; email: christine.eischen@jefferson.edu

Keywords: Mtbp, Myc, aging, longevity, lymphoma

Received: July 15, 2016

Accepted: October 15, 2016

Published: October 30, 2016

ABSTRACT

Alterations of specific genes can modulate aging. Myc, a transcription factor that regulates the expression of many genes involved in critical cellular functions was shown to have a role in controlling longevity. Decreased expression of Myc inhibited many of the deleterious effects of aging and increased lifespan in mice. Without altering Myc expression, reduced levels of Mtbp, a recently identified regulator of Myc, limit Myc transcriptional activity and proliferation, while increased levels promote Myc-mediated effects. To determine the contribution of Mtbp to the effects of Myc on aging, we studied a large cohort of *Mtbp* heterozygous mice and littermate matched wild-type controls. Mtbp haploinsufficiency significantly increased longevity and maximal survival in mice. Reduced levels of Mtbp did not alter locomotor activity, litter size, or body size, but *Mtbp* heterozygous mice did exhibit elevated markers of metabolism, particularly in the liver. *Mtbp*^{+/-} mice also had a significant delay in spontaneous cancer development, which was most prominent in the hematopoietic system, and an altered tumor spectrum compared to *Mtbp*^{+/+} mice. Therefore, the data suggest Mtbp is a regulator of longevity in mice that mimics some, but not all, of the properties of Myc in aging.

INTRODUCTION

Aging is a complex biological process controlled by both environmental and genetic factors [1]; however, twin studies suggest 20-30% of lifespan variation is genetic [2, 3]. Altering the activity or expression of specific genes significantly impacts lifespan in animal models [4]. For example, increased expression of the protein deacetylase Sirt1 is known to slow the effects of aging and increase lifespan [5]. In contrast, reduced levels of the oncogenic transcription factor c-Myc (Myc), due to heterozygosity, was recently reported to significantly increase longevity in mice [6-8].

Myc is estimated to transcriptionally regulate 10-15% of the genome [9, 10]. While Myc has been implicated in processes such as stem cell maintenance, differentiation, and apoptosis, Myc transcriptional activity is closely linked to cell-cycle progression and the vast metabolic machinery required for cellular proliferation

[6, 7, 11]. Notably, Myc regulates mitochondrial biogenesis through expression of genes such as *Pgc1 α* and *Pgc1 β* (peroxisome proliferation activated receptor gamma coactivator 1-alpha and beta), providing sufficient mitochondria to maintain increased cellular metabolism [12]. Myc increases overall cellular energy flux by upregulating glycolysis and glutaminolysis through transcriptional activations of target genes like hexokinase 2 (*Hk2*) and glutaminase (Gls; [13-16]). The energy generated from these metabolic pathways is then utilized by downstream pathways regulated by Myc to generate critical macromolecules. For example, Myc regulates urea cycling and pyrimidine synthesis, via transcriptional regulation of ornithine decarboxylase (*Odc*) and carbamoyl-phosphate synthetase 2/aspartate transcarbamylase/dihydroorotase (*Cad*), respectively [17, 18]. Myc also increases overall protein synthesis [19], a known modulator of longevity [20], through regulation of genes like nucleolin (*Ncl*) that control ribosomal assembly [21].

Based on the broad control Myc exerts over cellular processes relevant to aging and the recent publication directly linking Myc to longevity [8], proteins that regulate Myc represent potential modulators of the aging process. We recently reported that Mtbp is a Myc transcriptional co-factor [22]. In mice, *Mtbp* heterozygosity resulted in reduced Mtbp protein expression without altering Myc levels, and this inhibited Myc-mediated transcriptional activation of target genes, proliferation, and B cell lymphoma development [23]. Knockdown of *Mtbp* expression delayed cell cycle progression through S and G2/M phases of the cell cycle [24, 25]. In contrast, elevated Mtbp expression increased the number of cells in S-phase and enhanced Myc-mediated transcription and tumor development [22]. These data indicate Mtbp is a positive regulator of Myc transcriptional activity and downstream biological functions. Thus, we tested whether reduced Mtbp expression would alter aging in similar ways to decreased Myc expression [8].

RESULTS

Mtbp^{+/-} mice have increased longevity

Since *Myc*^{+/-} mice have increased longevity [8] and we have shown that Mtbp is a positive regulator of Myc [22, 23], we investigated the contribution of Mtbp to longevity using a cohort of littermate-matched *Mtbp*^{+/+} and *Mtbp*^{+/-} mice. *Mtbp* heterozygous mice had increased longevity compared to wild-type controls, exhibiting a median survival of 785 days compared to 654 days ($p=0.0013$; Figure 1A, Supplemental Figure S1), a 20% increase. This significant difference in lifespan was represented in both male and female populations (Figure 1B and 1C). *Mtbp* heterozygous males had a median survival of 774 days, compared to 672 days for wild-type control males ($p=0.0166$, Supplemental Figure S1), a 15.2% increase. *Mtbp*^{+/-} females had a median survival of 790 days, compared to 650.5 days for *Mtbp*^{+/+} females ($p=0.0439$), a 21.4% increase (Supplemental Figure S1).

In addition to median lifespan, *Mtbp* heterozygosity also increased maximum lifespan. Specifically, *Mtbp*^{+/-} mice were overrepresented in the longest living decile and quartile of mice with 9 of 11 (81.8%) and 19 of 26 (73.1%) of the mice, respectively (Figure 1D). The trend was not affected by gender, as the longest living decile and quartile of mice were 4 of 5 (80.0%) and 9 of 12 (75.0%) heterozygous males, respectively, and 4 of 5 (80.0%) and 10 of 13 (76.9%) heterozygous females, respectively. In contrast, *Mtbp* wild-type mice (all mice and both male and female) were disproportionately represented in the shortest lived decile and quartile of mice 90.9% and 80.8%, respectively (Figure 1D). This

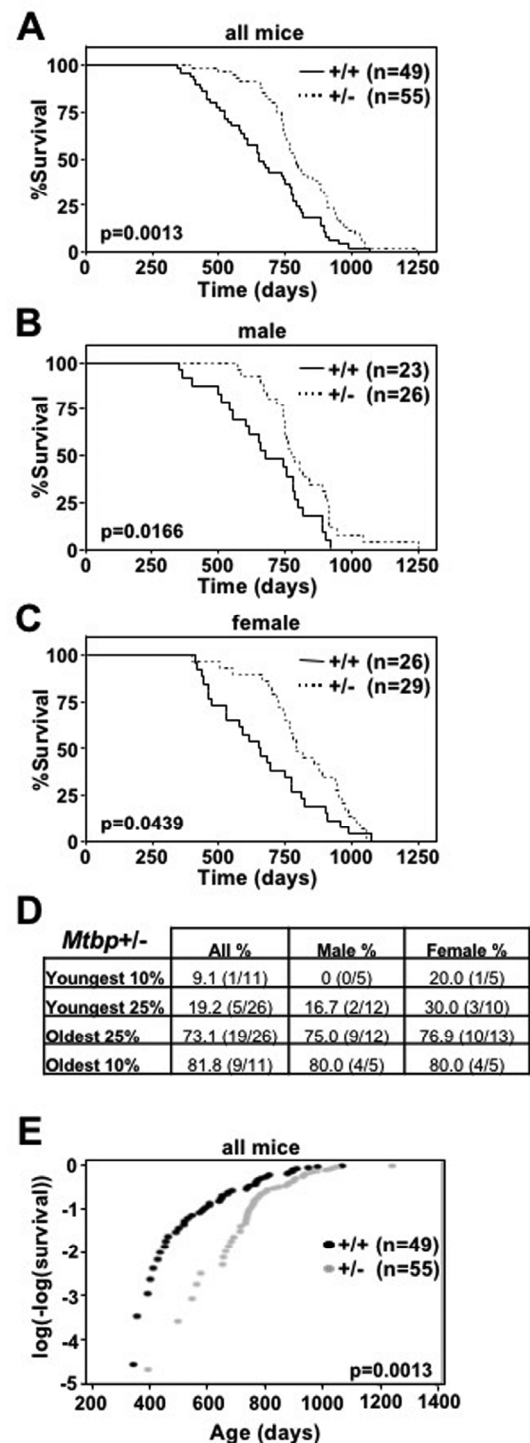


Figure 1. *Mtbp* heterozygosity increases longevity. (A-C) Kaplan-Meier survival curves of *Mtbp*^{+/+} (+/+) and *Mtbp*^{+/-} (+/-) mice with the number of mice in each group denoted by n. p value determined by log-rank tests. (D) All, male, and female *Mtbp*^{+/-} mice in the indicated decile or quartile of the mouse cohort. (E) Instantaneous death rate plotted; log-rank $p=0.0013$, Chi-sq=10.27, df=1; number of mice in each group denoted by n.

was also reflected in the observation that *Mtbp*^{+/-} mice have a significantly decreased instantaneous death rate

compared to *Mtbp*^{+/+} littermate-matched controls (log-rank p=0.0013, Chi-sq=10.27, df=1; Figure 1E). Both *Mtbp* heterozygous males and females have a significantly reduced instantaneous death rate (log-rank p=0.0166, Chi-sq=5.74, df=1 and log-rank p=0.0439, Chi-sq=4.06, df=1, respectively; Supplemental Figure S2). Therefore, an *Mtbp* haploinsufficiency confers increased median and maximum survival.

Delay in tumorigenesis and a change of tumor spectrum in *Mtbp* heterozygous mice

As is commonly seen in C56Bl/6 mice [26, 27], gross and histopathological tissue analysis at time of death of representative mice demonstrated the majority had cancer (17 of 23 *Mtbp*^{+/+} mice and 29 of 34 *Mtbp*^{+/-} mice). Notably, 32.4% (11 of 34) of *Mtbp*^{+/-} mice had lymphoma, which was twice the incidence of lymphoma in *Mtbp*^{+/+} mice (17.4%, 4 of 23; Figure 2A). The lymphomas were detected at an average age of 840 days in heterozygotes, compared to 682.3 days in wild-type controls, a significant delay (p=0.0320, Supplemental Figure S1). Similarly, *Mtbp*^{+/-} mice developed carcinomas later in life at 848 days (3 of 34, 8.8%) compared to 694 days for *Mtbp*^{+/+} mice (3 of 23, 13.0%) and the tissue distribution of the carcinomas differed between the two genotypes. Specifically, two carcinomas that developed in the wild-type mice were hepatocellular carcinoma and one was a carcinoma of the small intestine, whereas two of the *Mtbp* heterozygous mice developed aural squamous cell carcinoma and one had pulmonary adenocarcinoma. The difference in age of carcinoma development and the type of carcinoma that emerged between the two genotypes was not statistically significant likely due to the small number of carcinomas that developed (p=0.1412; Supplemental Figure S1, Figure 2B). In contrast, *Mtbp*^{+/+} and *Mtbp*^{+/-} mice had a similar frequency and

age of onset of sarcoma. Approximately half of the cancers that developed in both genotypes of mice were sarcoma [10 of 23 (43.5%) for *Mtbp*^{+/+} and 15 of 34 (44.1%) for *Mtbp*^{+/-}; Figure 2C], occurring at a mean age of 806 days for *Mtbp*^{+/+} and 743 days for *Mtbp*^{+/-} mice (p = 0.1547, Supplemental Figure S1). The vast majority of the sarcomas in both the wild-type and *Mtbp* heterozygous mice were histiocytic sarcomas. One *Mtbp* wild-type mouse developed both a sarcoma and a carcinoma, and all *Mtbp*^{+/-} mice that were diagnosed with a malignancy had only one tumor type. Although, twice the proportion of *Mtbp* wild-type control mice were cancer free at time of death (7 of 23, 30.4%) compared to *Mtbp* heterozygous mice (5 of 34, 14.7%; Figure 2D), the *Mtbp*^{+/-} mice lived an average of 836.4 days compared to 640.3 days for wild-type controls (Supplemental Figure S1). This difference in *Mtbp*^{+/-} mice represents a significant delay in mortality among cancer free mice (p=0.03340). These data collectively indicate a decrease in *Mtbp* expression alters the tumor spectrum and age of onset as mice age, as well as extends overall survival independent of cancer development.

Mtbp^{+/+} and *Mtbp*^{+/-} mice move, reproduce, and develop similarly

Long-lived mouse models will often retain elevated motor function compared to controls, particularly as they age. To determine if *Mtbp* heterozygosity improved locomotor activity, open field testing was performed for 1 hour on two days with a cohort of old (1.5 year) littermate matched mice. Although there was a trend for *Mtbp* heterozygotes to travel a greater distance (5737.7 cm) compared to wild-type controls (4551.0 cm), this difference did not reach statistical significance (p=0.1142; Figure 3A). When locomotor function was actively challenged using a rota-rod en-

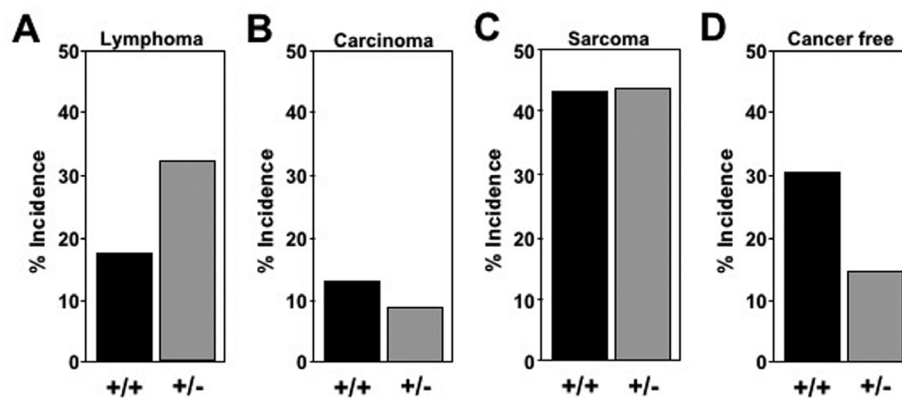


Figure 2. Altered tumor spectrum in *Mtbp*^{+/-} mice. Pathological/histological evaluation of tissues at time of death of *Mtbp*^{+/+} n=23 and *Mtbp*^{+/-} n=34 littermates analyzed. The percentage of mice with each diagnosis plotted (A-D).

duration test, the *Mtbp*^{+/-} mice (78.0 seconds) performed similarly to *Mtbp*^{+/+} mice (73.6 seconds) after training (Figure 3B; p=0.3923). Analogous results were also obtained with younger mice (Supplemental Figure S3).

In nature, many animal species with increased longevity have reduced reproductive capacity to limit overpopulation. This trend has been reported in some long-lived mouse models [28]. Thus, we compared the reproductive efficiency of *Mtbp*^{+/+} and *Mtbp*^{+/-} female

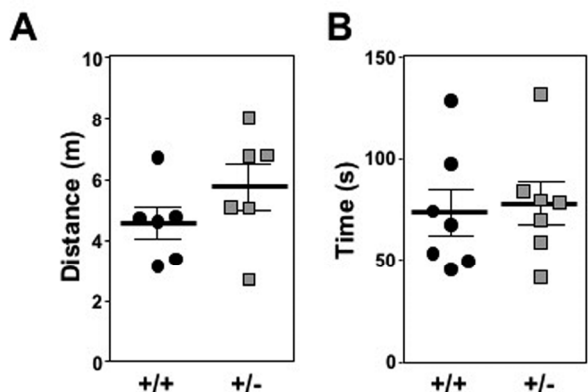


Figure 3. *Mtbp* heterozygosity does not significantly alter locomotor activity in old mice. (A) *Mtbp*^{+/+} (+/+; circle) and *Mtbp*^{+/-} (+/-; square) mice were placed in an open field cage and the total distance traveled in one hour was recorded using a laser grid and averaged for two consecutive days (p=0.1142). (B) After two days of training, the time mice spent on an accelerating rotarod was recorded and averaged from three consecutive trials separated by 10 minutes of rest (p=0.3923). P values calculated with student's t-tests and error bars are SEM.

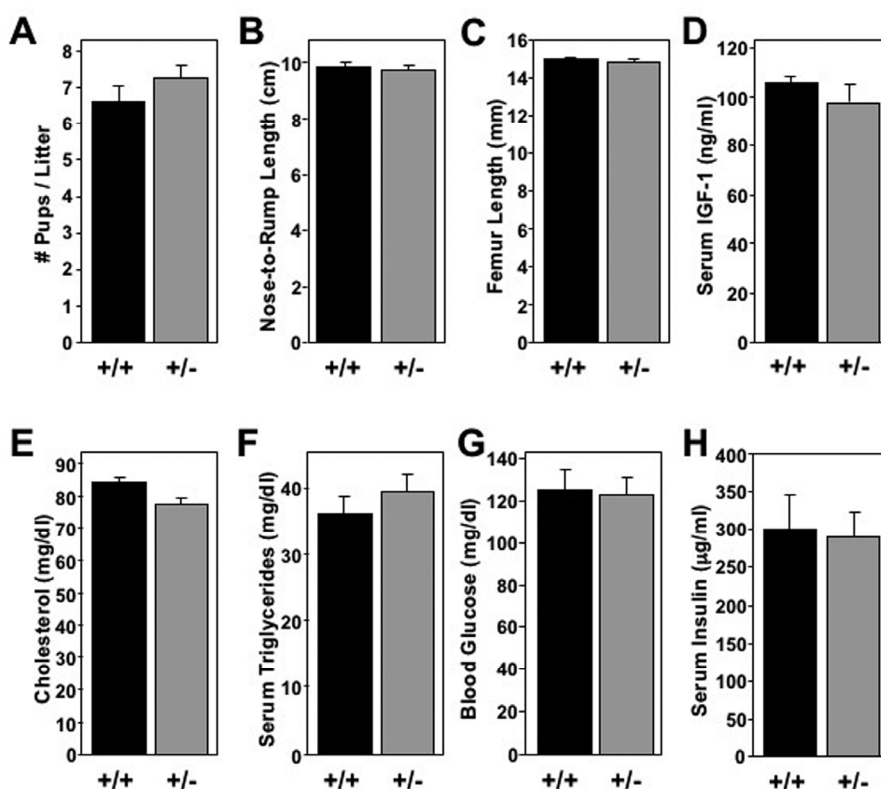


Figure 4. Long-lived *Mtbp* heterozygous mice exhibit normal systemic physiology. (A) The mean number of pups birthed from *Mtbp*^{+/+} × *Mtbp*^{+/-} crosses by each female *Mtbp*^{+/+} (+/+; n=20 females; 328 total pups; black) and *Mtbp*^{+/-} (+/-; n=25 females; 569 total pups; gray) mouse was recorded and averaged (p=0.2247). (B-H) Healthy long-lived (29 months) +/+ (n=5) and +/- (n=8) male mice were starved for 5 hours. (B) The nose-to-rump length was recorded and averaged (p=0.9999). (C) After sacrifice, the femurs were isolated and their length measured with electronic calipers and averaged (p=0.7160; n=7 for +/- group due to loss of one femur from bilateral fracture from collection). (D-H) Blood was collected and serum isolated. Circulating levels of (D) IGF-1 (p=0.4175), (E) cholesterol (p=0.3572), (F) triglycerides (p=0.4037), (G) blood glucose (p=0.7116) and (H) insulin (p=0.6963) were measured. P values calculated with student's t-tests, and error bars are SEM.

mice. Only the number of pups per birth from crosses between *Mtbp*^{+/+} and *Mtbp*^{+/-} mice were quantified, as deletion of *Mtbp* is embryonic lethal and would artificially lower the number of pups birthed [29]. This examination did not reveal a significant difference in the average number of pups per litter birthed by *Mtbp*^{+/+} (6.6) and *Mtbp*^{+/-} (7.3) females (p=0.2247; Figure 4A).

Some long-lived mouse models reported to have reduced growth, resulting in smaller body size [30]. We detected no size differences in mature *Mtbp*^{+/-} mice. Specifically, *Mtbp*^{+/+} and *Mtbp*^{+/-} mice had similar nose-to-rump lengths of 9.89 cm and 9.74 cm, respectively (p=0.9999; Figure 4B) as well as femur lengths of 15.0 mm and 14.8 mm, respectively (p=0.7160; Figure 4C) at the time of sacrifice. Given this observation, it was not surprising that analysis of serum isolated and frozen at time of sacrifice did not show a statistically significant difference in the level of circulating insulin-like growth factor-1

(IGF-1; p=0.4175; Figure 4D), a major growth-promoting factor [31]. Therefore, an *Mtbp* haploinsufficiency did not impact locomotion, birth rates, or bone size.

Long-lived *Mtbp*^{+/-} mice exhibit signs of increased cellular metabolism

Many long-lived mouse models have changes in metabolism detectable at a systemic level. To determine if *Mtbp* expression modulates levels of circulating metabolic markers, serum was isolated and frozen immediately after sacrifice of long-lived mice starved for 5 hours. The analysis revealed *Mtbp*^{+/+} and *Mtbp*^{+/-} mice had similar levels of serum cholesterol (p=0.3572; Figure 4E) and triglycerides (p=0.4037; Figure 4F). Moreover, the circulating level of glucose (p=0.7116; Figure 4G) and insulin (p=0.6963; Figure 4H) were also similar, reflecting no major changes in physiologic glucose regulation.

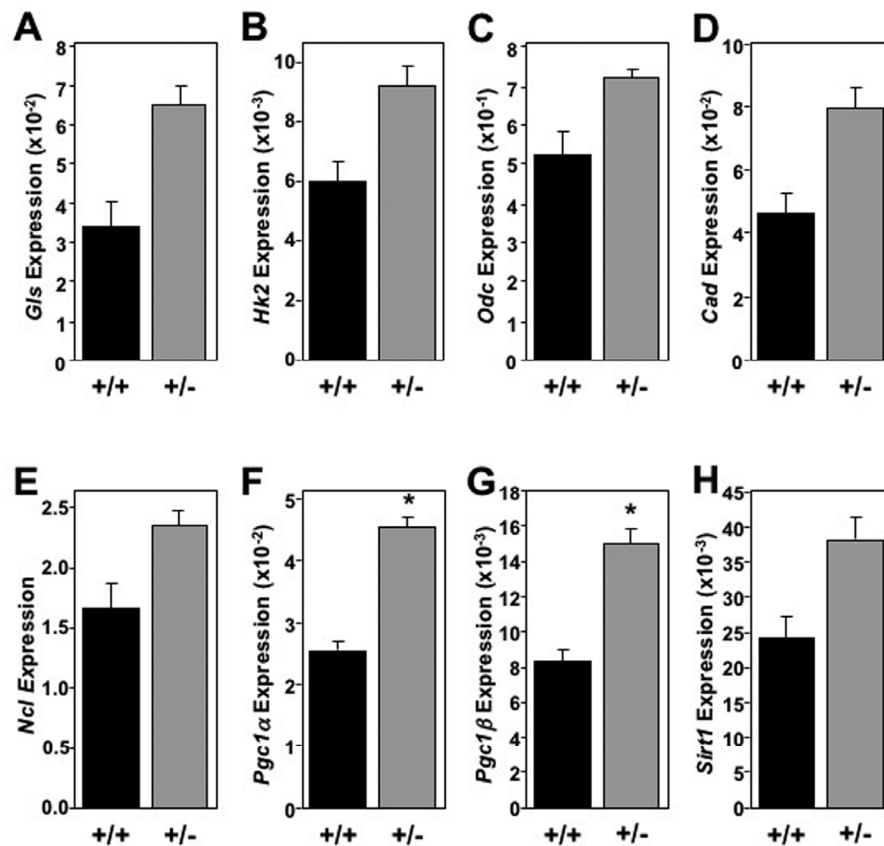


Figure 5. Old *Mtbp* heterozygous mouse livers exhibit global elevated metabolic markers. (A-H) Healthy *Mtbp*^{+/+} (+/+; n=5; black) and *Mtbp*^{+/-} (+/-; n=9; gray) mice at 29 months were starved for 5 hours, sacrificed, and livers frozen with Wallenburg clamp. qRT-PCR for (A) glutaminase (*Glis*, p=0.1147), (B) hexokinase 2 (*Hk2*, p=0.1401), (C) ornithine decarboxylase (*Odc*, p=0.0736), (D) carbamoyl-phosphate synthetase 2/aspartate transcarbamylase/dihydroorotase, (*Cad*, p=0.1393), (E) nucleolin (*Ncl*, p=0.1412), (F) peroxisome proliferation activated receptor gamma coactivator 1-alpha (*Pgc1α*, *p=0.0106), (G) *Pgc1*-beta (*Pgc1β*, *p=0.0499), and (H) sirtuin-1 (*Sirt1*, p=0.1529) was performed. Values are relative to β -actin levels. P values calculated using student's t-tests and error bars are SEM.

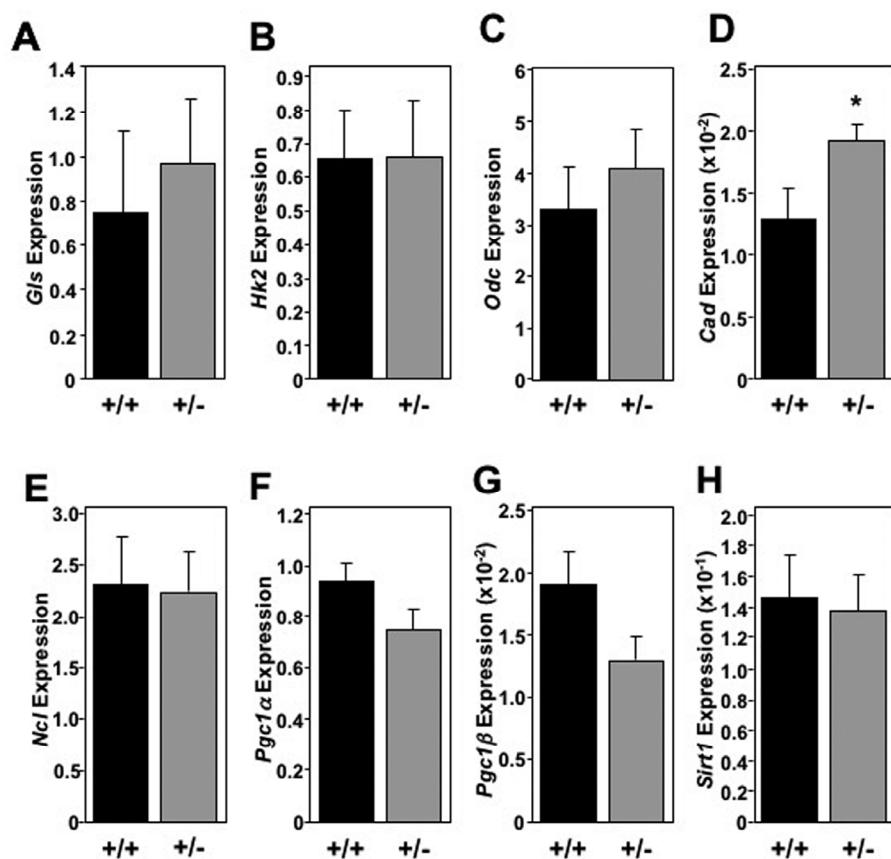


Figure 6. Skeletal muscle in old *Mtbp*^{+/-} mice lack global metabolic marker increase. (A-H) Healthy *Mtbp*^{+/+} (+/+; n=5; black) and *Mtbp*^{+/-} (+/-; n=8; gray) mice at 29 months were starved for 5 hours, sacrificed, and gastrocnemius muscle frozen with Wallenburg clamp. qRT-PCR for (A) glutaminase (*Gls*, p=0.5591; +/- n=7 due to RNA loss), (B) hexokinase 2 (*Hk2*, p=0.9792), (C) ornithine decarboxylase (*Odc*, p=0.5115), (D) carbamoyl-phosphate synthetase 2/aspartate transcarbamylase/dihydroorotase, (*Cad*, *p=0.0202), (E) nucleolin (*Ncl*, p=0.9116, +/- n=7 due to insufficient RNA), (F) peroxisome proliferation activated receptor gamma coactivator 1-alpha (*Pgc1α*, p=0.0736), (G) *Pgc1*-beta (*Pgc1β*, p=0.0710), and (H) sirtuin-1 (*Sirt1*, p=0.8417) was performed. Values are relative to *β-actin* levels. P values calculated using student's t-tests and error bars are SEM.

Although systemic changes in cholesterol, triglyceride, and glucose metabolism were not observed, we examined markers of cellular metabolism in tissues of long-lived mice to determine if decreased *Mtbp* expression modulates metabolism at a molecular level. Using flash frozen tissue at the time of sacrifice, mRNA was isolated from the liver, skeletal muscle (gastrocnemius) and brown fat pad of long-lived mice. In the liver, *Mtbp*^{+/-} mice exhibited a global trend toward, and at times significantly, increased expression of metabolic markers (Figure 5), similar to previous reports for *Myc*^{+/-} mice [8]. *Mtbp* heterozygosity resulted in a trend toward increased expression of basic metabolic genes such as *Gls*, *Hk2*, *Ncl*, *Cad*, and *Odc* that control cellular energy flux, protein translation, and macromolecule synthesis (Figure 5A-E). Most notably, the livers of *Mtbp*^{+/-} mice showed a nearly 2-fold and statistically significant increase in the expression of

Pgc1α (p=0.0106; Figure 5F) and *Pgc1β* (p = 0.0499; Figure 5G) compared to wild-type controls. This increase suggests elevated mitochondrial biogenesis and function in long-lived *Mtbp* heterozygous mice. These increased levels of metabolic markers in *Mtbp*^{+/-} livers also coincided with a nearly 60% increase in the expression of *Sirt1* (p=0.1529; Figure 5H), a well-known anti-aging gene linked to caloric restriction [32].

The global increase in metabolic markers observed in the livers of *Mtbp* heterozygous mice was largely not recapitulated in skeletal muscle (Figure 6) and brown fat (Figure 7). In skeletal muscle for example, there was only a statistically significant increase in the level of *Cad* in *Mtbp*^{+/-} mice (p=0.0202), but analogous levels of *Gls*, *Hk2*, *Odc*, and *Ncl* compared to *Mtbp*^{+/+} mice (Figure 6A-E). There was a trend toward significantly decreased expression of *Pgc1α* (p=0.0736; Figure 6F)

and *Pgc1β* ($p=0.0710$; Figure 6G), but similar levels of *Sirt1* (Figure 6H) in *Mtbp* heterozygous skeletal muscle. In brown fat, levels of *Gls*, *Hk2*, *Odc*, *Cad*, and *Ncl* were similar between wild-type and heterozygous *Mtbp* mice (Figure 7A-E). However, the brown fat of *Mtbp*^{+/-} mice exhibited a trend toward increased expression of *Pgc1α* ($p=0.0531$; Figure 7F), but equivalent levels of *Pgc1β* ($p=0.8492$; Figure 7G). The levels of *Sirt1* were analogous between the two genotypes (Figure 7H). Therefore, the data show *Mtbp* heterozygosity alters markers of cellular metabolism in disparate tissues, although the effects are more pronounced in the liver.

DISCUSSION

We reported that *Mtbp* is a positive regulator of *Myc* transcriptional activity, promoting *Myc*-mediated proliferation and malignant transformation [22, 23]. Yet, it was unclear if *Mtbp* expression contributed to *Myc*-modulation of aging that was recently reported [8]. Here, we determined *Mtbp* heterozygosity, like *Myc*

heterozygosity, significantly increased the median and maximum lifespan of mice and delaying cancer development compared to wild-type littermate-matched controls. The increase was observed regardless of gender. These results indicate *Mtbp* has a significant role in aging.

While cancer was the cause of death in the majority of mice, reduced *Mtbp* expression was associated with an increased, but significantly delayed, incidence of lymphoma. We observed a similar delay in lymphoma development in *Eμ-myc* transgenic mice that were *Mtbp*^{+/-} [23]. Interestingly, *Myc*^{+/-} mice, also had an increase in the rate of lymphoma, although to a much less degree, along with significantly reduced progression of disease at time of death [8]. In addition to delayed lymphoma development, there was also a trend for *Mtbp*^{+/-} mice to have delayed carcinoma development. However, *Mtbp* heterozygous and wild-type mice had a similar age of onset of sarcoma development. Therefore, the development of specific

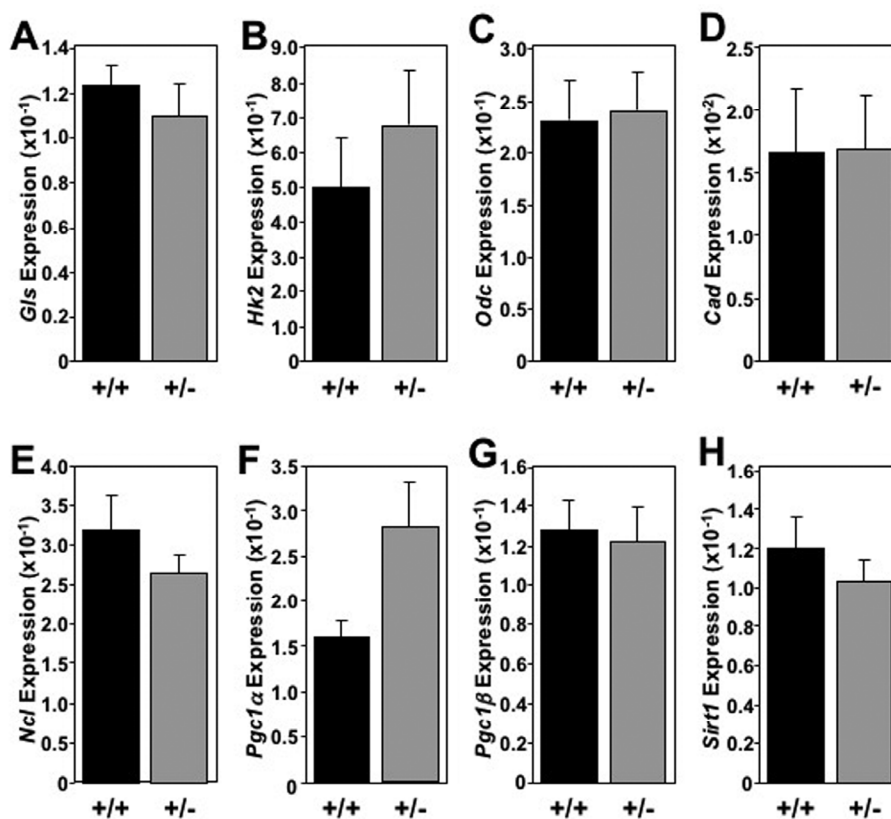


Figure 7. Absence of global elevation of metabolic markers in brown fat in old *Mtbp* heterozygous mice. (A-H) Healthy *Mtbp*^{+/+} (+/+; n=5; black) and *Mtbp*^{+/-} (+/-; n=8; gray) mice at 29 months were starved for 5 hours, sacrificed, and brown fat frozen. qRT-PCR for (A) glutaminase (*Gls*, $p=0.4982$), (B) hexokinase 2 (*Hk2*, $p=0.4555$), (C) ornithine decarboxylase (*Odc*, $p=0.8677$), (D) carbamoyl-phosphate synthetase 2/aspartate transcarbamylase/dihydroorotase, (*Cad*, $p=0.9700$), (E) nucleolin (*Ncl*, $p=0.2668$), (F) peroxisome proliferation activated receptor gamma coactivator 1-alpha (*Pgc1α*, $p=0.0531$), (G) *Pgc1*-beta (*Pgc1β*, $p=0.8492$, +/+ n=4 due to insufficient RNA), and (H) sirtuin-1 (*Sirt1*, $p=0.4146$) was performed. Values are relative to β -actin levels. P values calculated using student's t-tests and error bars are SEM.

cancer types appears to be more impacted than others by *Mtbp* heterozygosity. Specifically, the data suggest the hematopoietic compartment may be more sensitive to changes in *Mtbp* expression than other tissues. However, in human cancer, *MTBP* is amplified and/or overexpressed in a range of malignancies, including lymphomas, carcinomas, and sarcomas, suggesting it is oncogenic in multiple tissue types [22, 23, 33]. Future studies of *Mtbp* function comparing different normal and cancerous tissues should clarify those cell types in which altered *Mtbp* levels have a significant impact.

Our data that sarcomas present at a similar age suggest the overall survival difference between *Mtbp*^{+/-} and *Mtbp*^{+/+} mice does not appear to be due to an overall delay in cancer development. Additionally, fewer *Mtbp*^{+/-} mice were cancer-free at the time of death, a result not predicted had *Mtbp* only impacted longevity by decreasing and/or delaying cancer development. Notably, cancer-free *Mtbp*^{+/-} mice lived significantly longer than their cancer-free wild-type littermates, suggesting that in the absence of cancer, reduced *Mtbp* expression conferred a survival benefit. These data suggest that the delayed presentation of lymphoma may reflect increased vitality of the *Mtbp*^{+/-} mice, as lymphoma development occurred at younger ages in the wild-type cohort.

In addition to increased longevity and modulated cancer development, long-lived *Mtbp* heterozygous mice exhibited a global trend toward elevated cellular metabolism in the liver. While this may coincide with an overall increase in metabolism reported for *Myc*^{+/-} mice [8], specific ties to aging have also been described. For example, caloric restriction, well known to improve longevity, has been previously shown to increase hepatic *Gls* expression [34]. *Odc* expression is elevated in younger livers and been implicated in the capacity for hepatic repair and regeneration [35]. We also observed increased expression of *Pgc1α* and *Pgc1β*, which regulate mitochondrial biogenesis and function. Their reduced expression with aging has been associated with many age-related pathologies [36]. Collectively, increased expression of these metabolic markers suggests retained vitality in the livers of old *Mtbp*^{+/-} mice, which coincides with the elevated expression of the well-known anti-aging gene *Sirt1* [5].

The increased expression of metabolic genes observed in aged *Mtbp*^{+/-} livers was largely sporadic or nearly absent in skeletal muscle and brown fat. Interestingly, the absence of global metabolic changes in the skeletal muscle and brown fat of *Mtbp*^{+/-} mice compared to the global increase observed in the liver also matches with a lack of elevated *Sirt1* expression observed in these tissues. Moreover, the lack of increase in metabolic

markers and the downward trend in *Pgc1α* and *Pgc1β* expression in skeletal muscle of *Mtbp*^{+/-} mice support their similar performance in open field and rota-rod testing compared to wild-type controls. This is in contrast to *Myc*^{+/-} mice, which showed metabolic changes in skeletal muscle and improved rota-rod performance [8]. The reasons for the differential response to decreased *Mtbp* expression in the liver compared to skeletal muscle and adipose tissue is unclear at this time. However, a microarray analysis of liver, skeletal muscle, and adipose tissue in old *Myc*^{+/+} and *Myc*^{+/-} revealed the highest number of differentially expressed genes occurred in the liver [8]. Thus, future studies focused on the tissue-specific benefits of reduced *Mtbp* and/or *Myc* expression would be important.

Collectively, the data suggest *Mtbp* impacts longevity and cellular metabolism, particularly in the liver. These results are in line with a recent report on *Myc* [8] as well as our previous reports indicating *Mtbp* is a positive regulator of *Myc* transcriptional activity [22, 23]. However, the effect of *Myc* heterozygosity appears broader than the effects observed for *Mtbp* heterozygosity. For example, decreased *Myc* expression resulted in smaller body size, improved rota-rod performance, reduced circulating IGF-1, and lower serum cholesterol [8]. The precise reason for these differences is unclear at this time, although we have previously demonstrated *Mtbp* expression does not alter protein expression of *Myc* [22, 23], but did change the transcriptional activity of *Myc*. Part of the downstream effects of *Myc* are mediated through direct binding to or displacement of other factors at DNA, such as Miz1, NFY, C/EBPβ, SP1, and Foxo3A [7, 37, 38]. *Myc* also regulates transcriptional elongation through recruitment of P-TEFb [39, 40]. It is unknown how *Mtbp* expression impacts these functions of *Myc* or whether these functions of *Myc* change as animals age. Moreover, it is possible *Mtbp* may only orchestrate a sub-set of *Myc*'s overall transcriptional activity and may have *Myc*-independent functions. Therefore, additional research is needed on the interaction between *Mtbp* and *Myc*, and *Mtbp* itself, to better understand the contribution of *Mtbp* to aging.

METHODS

Mice

Mtbp^{+/-} [29] and littermate-matched *Mtbp*^{+/+} C57Bl/6 mice of both genders were generated through interbreeding and were housed together. For survival analysis, mice were sacrificed after meeting humane end-of-life criteria. Necropsy with tissue collection was performed and tissues were evaluated by a board-

certified veterinary pathologist (K.B.) in a blinded manner. For analysis of healthy aged mice (29 months-old), the mice were starved for 5 hours and crown-to-rump length was measured. Blood was collected and analyzed for blood glucose levels with Accu-chek test strips (Roche Diagnostics, Indianapolis, IN, USA; [41], centrifuged and plasma frozen for later analysis. Mice were sacrificed by cervical dislocation. Liver and gastrocnemius muscle were frozen with a Wallenburg clamp pre-cooled in liquid nitrogen as previously described [42]. Brown fat pads were collected and frozen. Tissues were kept at -80°C until analysis. Femurs were collected and measured with electronic calipers. Experiments were approved by the Vanderbilt Institutional Animal Care and Use Committee and followed all federal and state rules and regulations.

Quantitative real-time PCR (RT-PCR)

Total RNA was isolated from frozen tissues, cDNA was generated, and qRT-PCR was performed as previously described [23]. Primer sequences are listed in supplemental material.

Serum analysis

Analysis of serum was performed by the Mouse Metabolic Phenotyping Center in the Hormone Assay and Analytical Services and the Lipids and Lipoproteins Subcores at Vanderbilt University. Insulin levels were measured with a radioimmunoassay (SRI-13K, EMD Millipore, Billerica, MA, USA). IGF-1 levels were measured using a magnetic Luminex screening assay (LXSAMSM-01, R&D Systems, Minneapolis, MN, USA). Triglyceride and cholesterol levels were measured using Raichem reagents (R80035 and R84098, Cliniqua, San Marco, CA, USA).

Locomotion analysis

Explorative locomotion or open field testing was performed using a 48 channel IR controller (ENV-520, Med Associates Inc., St. Albans, Vermont) on young (6 months-old) and aged (21 months-old) mice. On two different days, mice were placed in the open field, the total distance traveled was recorded for 1 hour and the average of the two measurements was reported. Additionally, on three consecutive days, mice were placed on a five-lane accelerating rota-rod (47600, Ugo Basile, Varese, Italy) for three sequential trials separated by 10 minutes of rest. The rota-rod accelerated from 4 to 40 rpm over 3 minutes with a cut-off time of 3 minutes. Time running on the rota-rod was determined by using pressure sensors to detect falls or by observing >3 consecutive rotations of the mouse

around the rod. The average times from day 3 were recorded [43].

Statistical evaluation

A log-rank test was used to calculate significance in Figure 1 and Supplemental Figure S1. Analysis for Figure 1E and Supplemental Figure S1 was performed with JMP statistical software (v12.2.0). Student's t-test was used to calculate significance for data in Figures 2-7 and Supplemental Figures S2 and S3.

ACKNOWLEDGEMENTS

We thank Jessica Odvody and Pia Maria Arrate for technical assistance; Dr. Owen McGuinness for metabolic testing advice; Drs. Ron Emeson and John Allison for locomotor testing advice and planning; Dr. Dan Moore and Blair Stocks for material assistance with glucose monitoring; Dr. Alyssa Hasty for brown fat harvesting training; members of the Eischen lab for helpful discussion and review of the manuscript.

FUNDING

These studies were supported by F30AG039164 (BCG), T32GM007347 (BCG), R01CA148950 (CME), the NCI Cancer Center Support Grant P30CA056036, the Mouse Metabolic Phenotyping Core supported in part by U24DK059637, and the NCI Cancer Center Support Grant P30CA068485 utilizing the Translational Pathology Shared Resources.

CONFLICTS OF INTEREST

The authors declare that they have no conflict of interest.

REFERENCES

1. Kuningas M, Mooijaart SP, van Heemst D, Zwaan BJ, Slagboom PE, Westendorp RG. Genes encoding longevity: from model organisms to humans. *Aging Cell*. 2008; 7:270–80. doi: 10.1111/j.1474-9726.2008.00366.x
2. Herskind AM, McGue M, Holm NV, Sørensen TI, Harvald B, Vaupel JW. The heritability of human longevity: a population-based study of 2872 Danish twin pairs born 1870-1900. *Hum Genet*. 1996; 97:319–23. doi: 10.1007/BF02185763
3. Skytthe A, Pedersen NL, Kaprio J, Stazi MA, Hjelmberg JV, Iachine I, Vaupel JW, Christensen K. Longevity studies in GenomEUtwin. *Twin Res*. 2003; 6:448–54. doi: 10.1375/136905203770326457

4. Ladiges W, Van Remmen H, Strong R, Ikeno Y, Treuting P, Rabinovitch P, Richardson A. Lifespan extension in genetically modified mice. *Aging Cell*. 2009; 8:346–52. doi: 10.1111/j.1474-9726.2009.00491.x
5. Wang Y. Molecular Links between Caloric Restriction and Sir2/SIRT1 Activation. *Diabetes Metab J*. 2014; 38:321–29. doi: 10.4093/dmj.2014.38.5.321
6. Meyer N, Penn LZ. Reflecting on 25 years with MYC. *Nat Rev Cancer*. 2008; 8:976–90. doi: 10.1038/nrc2231
7. Tansey WP. Mammalian MYC Proteins and Cancer. *New J Sci*. 2014; 757534.
8. Hofmann JW, Zhao X, De Cecco M, Peterson AL, Pagliaroli L, Manivannan J, Hubbard GB, Ikeno Y, Zhang Y, Feng B, Li X, Serre T, Qi W, et al. Reduced expression of MYC increases longevity and enhances healthspan. *Cell*. 2015; 160:477–88. doi: 10.1016/j.cell.2014.12.016
9. Dang CV, O'Donnell KA, Zeller KI, Nguyen T, Osthus RC, Li F. The c-Myc target gene network. *Semin Cancer Biol*. 2006; 16:253–64. doi: 10.1016/j.semcan.2006.07.014
10. O'Connell BC, Cheung AF, Simkevich CP, Tam W, Ren X, Mateyak MK, Sedivy JM. A large scale genetic analysis of c-Myc-regulated gene expression patterns. *J Biol Chem*. 2003; 278:12563–73. doi: 10.1074/jbc.M210462200
11. Dang CV. MYC, metabolism, cell growth, and tumorigenesis. *Cold Spring Harb Perspect Med*. 2013; 3:3. doi: 10.1101/cshperspect.a014217
12. Morrish F, Hockenbery D. MYC and mitochondrial biogenesis. *Cold Spring Harb Perspect Med*. 2014; 4:4. doi: 10.1101/cshperspect.a014225
13. Stine ZE, Walton ZE, Altman BJ, Hsieh AL, Dang CV. MYC, Metabolism, and Cancer. *Cancer Discov*. 2015; 5:1024–39. doi: 10.1158/2159-8290.CD-15-0507
14. Kim JW, Zeller KI, Wang Y, Jegga AG, Aronow BJ, O'Donnell KA, Dang CV. Evaluation of myc E-box phylogenetic footprints in glycolytic genes by chromatin immunoprecipitation assays. *Mol Cell Biol*. 2004; 24:5923–36. doi: 10.1128/MCB.24.13.5923-5936.2004
15. Wise DR, DeBerardinis RJ, Mancuso A, Sayed N, Zhang XY, Pfeiffer HK, Nissim I, Daikhin E, Yudkoff M, McMahon SB, Thompson CB. Myc regulates a transcriptional program that stimulates mitochondrial glutaminolysis and leads to glutamine addiction. *Proc Natl Acad Sci USA*. 2008; 105:18782–87. doi: 10.1073/pnas.0810199105
16. Gao P, Tchernyshyov I, Chang TC, Lee YS, Kita K, Ochi T, Zeller KI, De Marzo AM, Van Eyk JE, Mendell JT, Dang CV. c-Myc suppression of miR-23a/b enhances mitochondrial glutaminase expression and glutamine metabolism. *Nature*. 2009; 458:762–65. doi: 10.1038/nature07823
17. Miltenberger RJ, Sukow KA, Farnham PJ. An E-box-mediated increase in cad transcription at the G1/S-phase boundary is suppressed by inhibitory c-Myc mutants. *Mol Cell Biol*. 1995; 15:2527–35. doi: 10.1128/MCB.15.5.2527
18. Wagner AJ, Meyers C, Laimins LA, Hay N. c-Myc induces the expression and activity of ornithine decarboxylase. *Cell Growth Differ*. 1993; 4:879–83.
19. Brown SJ, Cole MD, Erives AJ. Evolution of the holozoan ribosome biogenesis regulon. *BMC Genomics*. 2008; 9:442. doi: 10.1186/1471-2164-9-442
20. Johnson SC, Rabinovitch PS, Kaeberlein M. mTOR is a key modulator of ageing and age-related disease. *Nature*. 2013; 493:338–45. doi: 10.1038/nature11861
21. Iritani BM, Eisenman RN. c-Myc enhances protein synthesis and cell size during B lymphocyte development. *Proc Natl Acad Sci USA*. 1999; 96:13180–85. doi: 10.1073/pnas.96.23.13180
22. Grieb BC, Gramling MW, Arrate MP, Chen X, Beauparlant SL, Haines DS, Xiao H, Eischen CM. Oncogenic protein MTBP interacts with MYC to promote tumorigenesis. *Cancer Res*. 2014; 74:3591–602. doi: 10.1158/0008-5472.CAN-13-2149
23. Odvody J, Vincent T, Arrate MP, Grieb B, Wang S, Garriga J, Lozano G, Iwakuma T, Haines DS, Eischen CM. A deficiency in Mdm2 binding protein inhibits Myc-induced B-cell proliferation and lymphomagenesis. *Oncogene*. 2010; 29:3287–96. doi: 10.1038/onc.2010.82
24. Boos D, Yekezare M, Diffley JF. Identification of a heteromeric complex that promotes DNA replication origin firing in human cells. *Science*. 2013; 340:981–84. doi: 10.1126/science.1237448
25. Agarwal N, Tochigi Y, Adhikari AS, Cui S, Cui Y, Iwakuma T. MTBP plays a crucial role in mitotic progression and chromosome segregation. *Cell Death Differ*. 2011; 18:1208–19. doi: 10.1038/cdd.2010.189
26. Pettan-Brewer C, Treuting PM. Practical pathology of aging mice. *Pathobiol Aging Age Relat Dis*. 2011; 1:1. doi: 10.3402/pba.v1i0.7202
27. Frith CH, Highman B, Burger G, Sheldon WD. Spontaneous lesions in virgin and retired breeder BALB/c and C57BL/6 mice. *Lab Anim Sci*. 1983; 33:273–86.

28. Lee C, Longo VD. Fasting vs dietary restriction in cellular protection and cancer treatment: from model organisms to patients. *Oncogene*. 2011; 30:3305–16. doi: 10.1038/onc.2011.91
29. Iwakuma T, Tochigi Y, Van Pelt CS, Caldwell LC, Terzian T, Parant JM, Chau GP, Koch JG, Eischen CM, Lozano G. Mtbp haploinsufficiency in mice increases tumor metastasis. *Oncogene*. 2008; 27:1813–20. doi: 10.1038/sj.onc.1210827
30. Anisimov VN, Arbeev KG, Popovich IG, Zabezhinski MA, Rosenfeld SV, Piskunova TS, Arbeeveva LS, Semenchenko AV, Yashin AI. Body weight is not always a good predictor of longevity in mice. *Exp Gerontol*. 2004; 39:305–19. doi: 10.1016/j.exger.2003.12.007
31. Stratikopoulos E, Szabolcs M, Dragatsis I, Klinakis A, Efstratiadis A. The hormonal action of IGF1 in postnatal mouse growth. *Proc Natl Acad Sci USA*. 2008; 105:19378–83. doi: 10.1073/pnas.0809223105
32. Bordone L, Guarente L. Calorie restriction, SIRT1 and metabolism: understanding longevity. *Nat Rev Mol Cell Biol*. 2005; 6:298–305. doi: 10.1038/nrm1616
33. Grieb BC, Chen X, Eischen CM. MTBP is overexpressed in triple-negative breast cancer and contributes to its growth and survival. *Mol Cancer Res*. 2014; 12:1216–24. doi: 10.1158/1541-7786.MCR-14-0069
34. Dhahbi JM, Mote PL, Wingo J, Tillman JB, Walford RL, Spindler SR. Calories and aging alter gene expression for gluconeogenic, glycolytic, and nitrogen-metabolizing enzymes. *Am J Physiol*. 1999; 277:E352–60.
35. Beyer HS, Ellefson M, Sherman R, Zieve L. Aging alters ornithine decarboxylase and decreases polyamines in regenerating rat liver but putrescine replacement has no effect. *J Lab Clin Med*. 1992; 119:38–47.
36. Wenz T. Mitochondria and PGC-1 α in Aging and Age-Associated Diseases. *J Aging Res*. 2011; 2011:810619. doi: 10.4061/2011/810619
37. Herkert B, Eilers M. Transcriptional repression: the dark side of myc. *Genes Cancer*. 2010; 1:580–86. doi: 10.1177/1947601910379012
38. Peck B, Ferber EC, Schulze A. Antagonism between FOXO and MYC Regulates Cellular Powerhouse. *Front Oncol*. 2013; 3:96. doi: 10.3389/fonc.2013.00096
39. Eberhardy SR, Farnham PJ. c-Myc mediates activation of the cad promoter via a post-RNA polymerase II recruitment mechanism. *J Biol Chem*. 2001; 276:48562–71.
40. Eberhardy SR, Farnham PJ. Myc recruits P-TEFb to mediate the final step in the transcriptional activation of the cad promoter. *J Biol Chem*. 2002; 277:40156–62. doi: 10.1074/jbc.M207441200
41. Wilson CS, Elizer SK, Marshall AF, Stocks BT, Moore DJ. Regulation of B lymphocyte responses to Toll-like receptor ligand binding during diabetes prevention in non-obese diabetic (NOD) mice. *J Diabetes*. 2016; 8:120–31. doi: 10.1111/1753-0407.12263
42. Chen SS, Otero YF, Mulligan KX, Lundblad TM, Williams PE, McGuinness OP. Liver, but not muscle, has an entrainable metabolic memory. *PLoS One*. 2014; 9:e86164. doi: 10.1371/journal.pone.0086164
43. Justice JN, Carter CS, Beck HJ, Gioscia-Ryan RA, McQueen M, Enoka RM, Seals DR. Battery of behavioral tests in mice that models age-associated changes in human motor function. *Age (Dordr)*. 2014; 36:583–92. doi: 10.1007/s11357-013-9589-9

SUPPLEMENTAL MATERIAL

METHODS

Real Time PCR Primers

Cad-F – AACTGCGTAGGCTTCGACCATACA
Cad-R – AATCAATGCGGGTGAGCTCGTAGA
Gls [1]
Gls-F – TTCGCCCTCGGAGATCCTAC
Gls-R – CCAAGCTAGGTAACAGACCCT
Hk2 [2]
Hk2-F – TGATCGCCTGCTTATTCACGG
Hk2-R – AACCGCCTAGAAATCTCCAGA
Ncl-F – ACTGGAAAGACCAGCACTTGGAGT
Ncl-R – CCCTTTAGGTTTGCCATGTGGGT
Odc-F – GCATGTGGGTGATTGGATGCTGTT
Odc-R – TTGCCACATTGGCCGTGACATTAC
Pcg1a-F – GGATGAATACCGCAAAGAGC
Pcg1a-R – GGTAGGTGATGAAACCATAGC
Pcg1b [3]
Pcg1b-F – TCCTGTAAAAGCCCGGAGTAT
Pcg1b-R – GCTCTGGTAGGGGCAGTGA
Sirt1 [4]
Sirt1-F – ACCTCCCAGACCCTCAAGC
Sirt1-R – TTCCTTCCTTATCTGACAAAGC

FIGURES

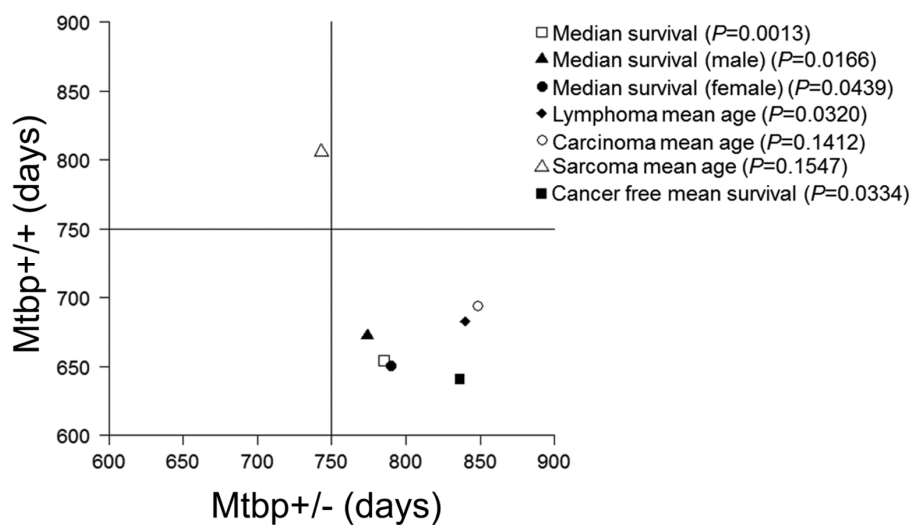


Figure S1. Indicators of increased longevity in *Mtbp+/-* mice. Ages of the events indicated in the key for *Mtbp+/-* mice compared to littermate matched *Mtbp+/-* mice plotted. P values determined by student's t-tests.

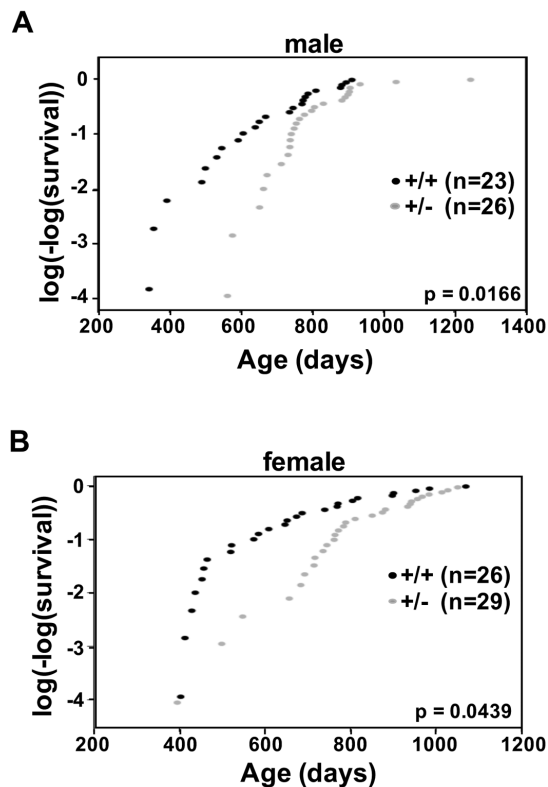


Figure S2. Male and female *Mtbp* heterozygous mice have a decreased instantaneous death rate. Instantaneous death rate plotted for males (A), log-rank $P = 0.0166$, Chi-sq=5.74, df=1) and females (B), log-rank $P = 0.0439$, Chi-sq=4.06, df=1). The number of mice in each group denoted by n.

REFERENCES

- Hettmer S, Schinzel AC, Tchessalova D, Schneider M, Parker CL, Bronson RT, Richards NG, Hahn WC and Wagers AJ. Functional genomic screening reveals asparagines dependence as a metabolic vulnerability in sarcoma. *Elife*. 2015; 4.
- Shi LZ, Wang R, Huang G, Vogel P, Neale G, Green DR and Chi H. HIF1 α dependent glycolytic pathway orchestrates a metabolic checkpoint for the differentiation of TH17 and Treg cells. *J Exp Med*. 2011; 208: 1367-1376.
- Walkey CJ and Spiegelman BM. A functional peroxisome proliferator-activated receptor- γ ligand-binding domain is not required for adipogenesis. *J Biol Chem*. 2008; 283: 24290-24294.
- Saini A, Al-Shanti N, Sharples AP and Stewart CE. Sirtuin 1 regulates skeletal myoblast survival and enhances differentiation in the presence of resveratrol. *Exp Physiol*. 2012; 97: 400-418.

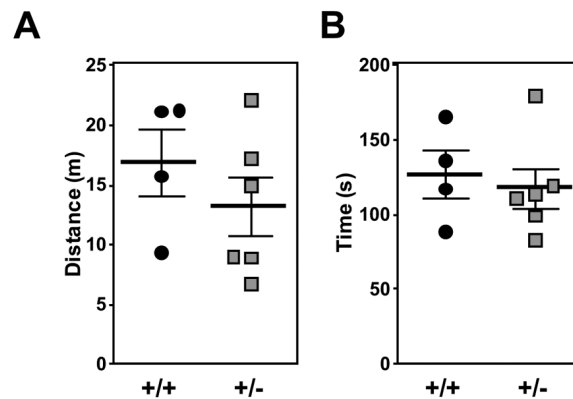


Figure S3. *Mtbp* heterozygosity does not significantly alter locomotor activity in young mice. (A) Six month-old *Mtbp*^{+/+} (+/+; circle) and *Mtbp*^{+/-} (+/-; square) mice were placed in an open field cage and the total distance traveled in one hour was recorded using a laser grid and averaged for two consecutive days ($p = 0.1772$). (B) After two days of training, the time +/+ and +/- mice spent on an accelerating rotarod recorded and averaged from three consecutive trials separated by 10 minutes of rest ($p=0.3359$). P values calculated with student's t-tests. Error bars represent standard error of the mean.